MATHEMATICAL MODELING AND SIMULATION FOR DETECTION OF SUICIDE BOMBERS

William P. Fox[(a)], John Vesecky[(b)], Kenneth Laws[(b)]

(a) Department of Defense Analysis, Naval Postgraduate School, Monterey, CA 993943
[(b)]Department of Electrical Engineering, University of California at Santa Cruz
[(a)] wpfox@nps.edu, [(b)]vesecky@cse.ucsc.edu, [(c)]kip@soe.ucsc.edu

ABSTRACT
We examined the use of radar to detect humans wearing a suicide bomb vest with detonation wires. In our research we used the GunnPlexer Doppler radar at 12.5 GHz to collect experiment data of humans both with wires and a vest and without wires. We collected data and broke the reflected radar signal into both horizontal and vertical polarization (HH and VV). We developed several metrics from this data that could be used in building models or algorithms to more accurately detect subjects wearing wires. We discovered additional information about the metrics and used combinations of the metrics so we could increase the detection probability. We built a Monte Carlo simulation to test our theories. To date, we have a success rate over 98% and a false positive rate of under approximately 2%. This research and the results encourage us to think that suicide bombers can be found prior to their detonation of their bombs at a safe range.

Keywords: military application, radar cross section, detection, suicide bomber

1. INTRODUCTION

Improvised Explosive Devices (IEDs) are a major problem in the world we face today (Meigs, 2007). A major IED concern is the suicide bomber. The suicide bomber generally does not present their action prior to the event and can more easily accomplish their goal. We examine the dynamics involved in the suicide bomber and possible detection strategies using a stand-off radar.

The general observational situation we consider is illustrated in figure 2, below. We see one or more radars observing a crowd of people of whom one or more have wires on their bodies. Those with wires might be terrorists who plan to explode their suicide bomb. We anticipate that the range from the radar to the people (or animals) under observation would be typically 50 to 100 meters. Our plan is to make observations with one or more radars (and likely other sensors as well, such as video surveillance cameras or thermal imaging). The results of these observations become the essential input data to our mathematical model that assesses the system's ability to detect *suspects* (persons suspected of harmful intent) from among a crowd of *subjects* who are largely harmless.

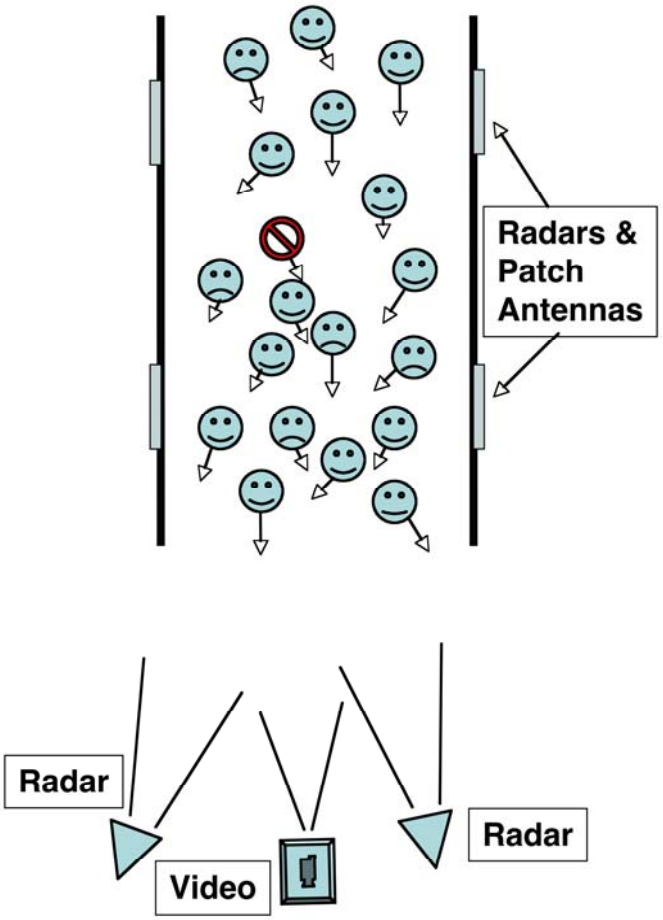

Figure 2. Radar observational geometry. One or more radars observe a group of people with one or two having wires on their bodies and hence becoming suspects.

We discuss the radar observational systems, the radar cross sections of humans both with and without wires on their bodies (from both experimental measurements and computational electromagnetic estimates), our mathematical models with metrics and our findings and conclusions with recommendations.

2. DETECTING SUICIDE BOMBERS

Data was collected using the GunnPlexer radar on persons both with and without wires & vests. This data has been analyzed. We begin by displaying the scatterplots, see Figure 1-3. Each plot indicates a visual exponential distribution. Using goodness of fit chi-squared analysis we found each does follow an exponential distribution.

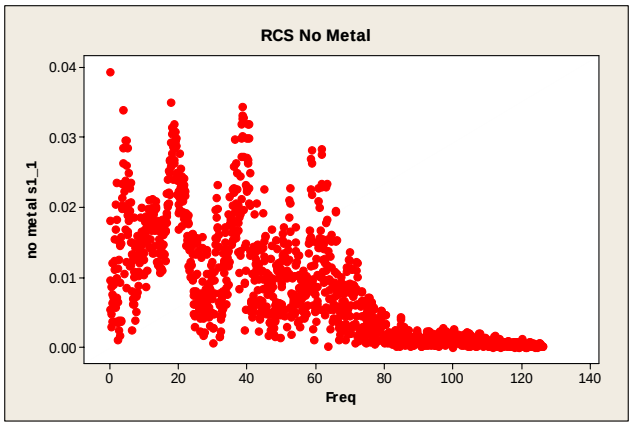

Figure 1. No wire on persons

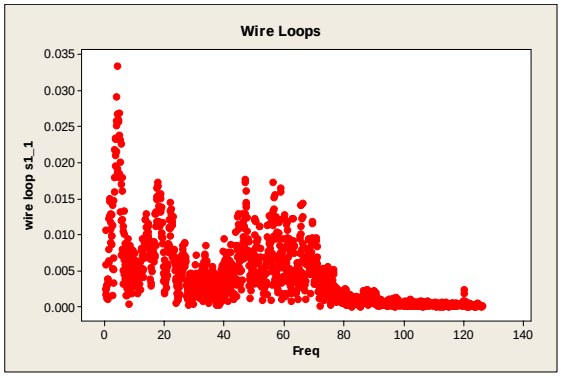

Figure 2. Persons wearing wire loops

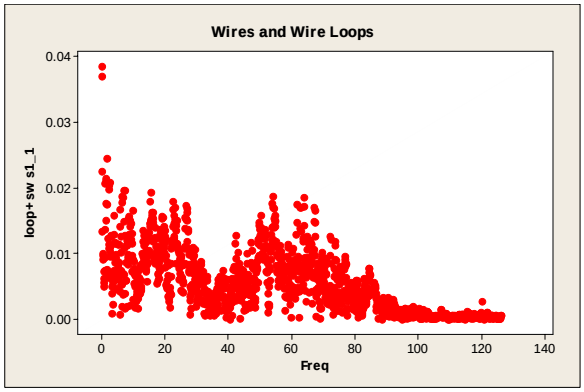

Figure 3. Person wearing wires and wire loops

Analysis of the data used to create these graphs show that each follows an exponential distribution. We used a Chi-squared goodness of fit test at α =0.05 for each test.

First, we took the scaled or normalized the data and then display a histogram of the data in Vest 1, see the figure 4 below.

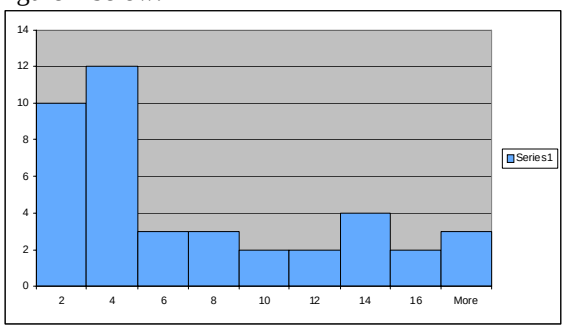

Figure 4. Histogram of Data set 1, Vest Configuration 1

We used the χ^2 goodness of fit test to a truncated exponential distribution:

$$H_0 : f(x) = \frac{\lambda e^{-\lambda x}}{1 - e^{-\lambda x_0}}, 0 \le x \le x_0$$

Since our test statistic value is less than my critical value then, we conclude that the truncated exponential with empirical mean 0 .15209355 is a good fit at an α level of 0.05

$$\chi^2 = 5.11619$$

$$\chi^2_{.05,4} = 9.48$$

We perform the same analysis for the data from Vest 2 seen in figure 5.

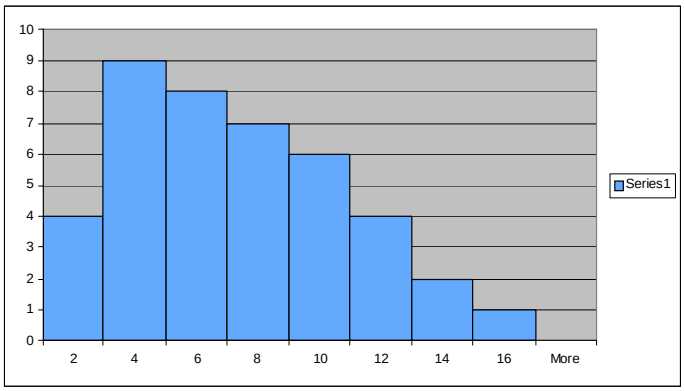

Figure 5. Histogram of data set 2, Vest Configuration 2

We tested using a goodness of fit test to a truncated exponential distribution:

$$H_0 : f(x) = \frac{\lambda e^{-\lambda x}}{1 - e^{-\lambda x_0}}, 0 \le x \le x_0$$

We conclude that the truncated exponential with empirical mean 0.156108622 is a good fit at an α level of 0.05.

$$\chi^2 = 4.6898$$
$$\chi^2_{.05,4} = 9.48$$

Both empirical distributions are essentially exponential distributions and that is supported by both the literature and other's research (Dogaru et al., 2007, Fox, et al, 2010, Angell et al. 2007a, 2007b).

We examined the vertical and horizontal polarization of the data that according to the literature might be able to distinguish certain objects. Linear polarization has been found to detect metal. We found that comparing the VV to HH polarization of our subjects was useful to identify metal. Our plots of the polarization data very closely resemble those of Dogaru et al. (2007), shown below in figure 6-7.

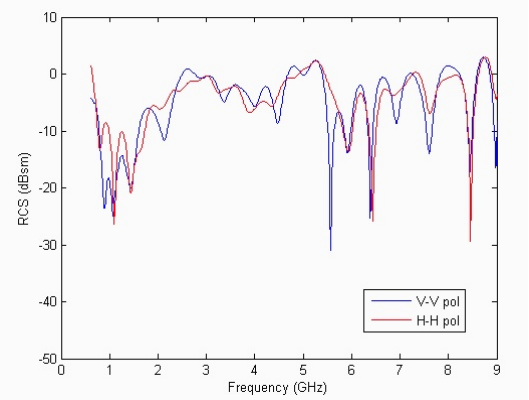

Figure 6. (Radar cross section of a simulated human body in both VV and HH polarization over the frequency range from 0.5 to 9 GHz. After Dogaru et al. (2007))

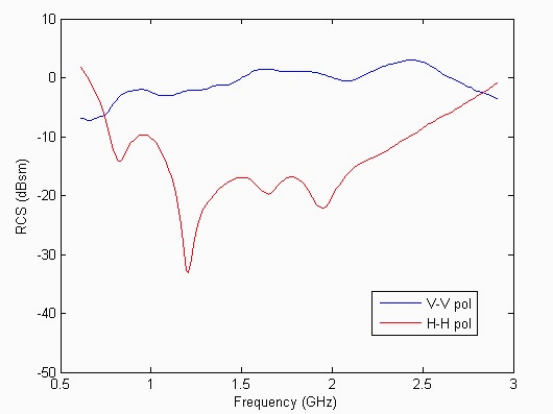

Figure 7. (Radar cross section of a human body carrying a thin, 1 m metal rod in front of the body. After Dogaru et al. (2007))

It is easy to see that the two figures are different. Figure 6 shows the two graphs (blue and red functions) and the plots are close to being the same. Figure 7 clearly shows visually that the two plots (blue and red) appear to be different. In fact, statistical analysis shows this is true. We analyzed two sets of data for person with wires in different arrays and tested the means in pairs to show they are different.

μ_1= mean for person with wires
μ_2= mean for person with wires (Vest 2)
μ_3= mean for persons with wires and loops (Vest 3)

Case 1:
$$H_0 : \mu_1 = \mu_2$$
$$H_a : \mu_1 \neq u_2$$

Case 2:
$$H_0 : \mu_1 = \mu_3$$
$$H_a : \mu_1 \neq u_3$$

Case 3:
$$H_0 : \mu_2 = \mu_3$$
$$H_a : \mu_2 \neq u_3$$

Rejection region with α =0.05 in each case is reject if |Z| > 1.96. The test statistics were found and are
Case 1: | Z | = |1.03-1.520/(0.1425)| = 3.439
Case 2: | Z | = |1.03-1.430/(0.1628)| = 2.457
Case 3: | Z | = |1.52-1.43/(0.186)| = 0.483

Our decisions from the hypothesis tests are:
Reject the null hypothesis in Case 1 and Case 2 concluding the ratios are different. we fail to reject the null hypothesis in Case 3, so we conclude the ratios for the wires on humans are statistically the same. This confirms they are different.

Previous results were weak in two areas (Fox, et al. 2010):

(1) our probability of detection was at most approximately 85% and
(2) our probability of false detections was high between 22-56%

We have created the wave forms of the polarization data using sinusoidal regression on the data in hopes of finding some new indicators. We obtained the following plots from the sinusoidal regression (Fox, 2011). Figure 8-12 show these results.

2.1 The Data

vvdata := [2.9981, 2.568, 3.334, 2.3511, 1.0501, 2.0599, 2.3896, 2.4332, 2.0329, 3.7039, 2.5939, 2.3927, 1.846, 1.6338, 1.259, 4.8333, 3.031, 2.4694, 1.0318, 0.88241, 3.8399, 6.7319, 4.7824,
1.3003, 1.896, 2.2515, 3.1435, 1.9894, 5.0677, 1.8283];

HHdata := [1.3997, 1.8211, 2.0562, 3.3373, 2.091, 1.4585, 3.2779, 0.98183, 1.2876, 0.75924, 0.79999, 2.2327, 3.3146, 3.7066, 1.6449, 1.7559, 1.3638, 2.665, 2.7001, 1.1329, 3.8667, 0.95611, 3.0781, 0.79202, 1.9711, 1.4571, 2.5922, 2.3116, 1.6376, 1.6722];

xdata := [1, 2, 3, 4, 5, 6, 7, 8, 9, 10, 11, 12, 13, 14, 15, 16, 17, 18, 19, 20, 21, 22, 23, 24, 25, 26, 27, 28, 29, 30];

nwvv := [−0.02289, 0.045738, 0.055329, 2.0421, 3.0388, 1.9826, 2.6181, 1.0328, 2.1586, 2.2184, 1.1283, 0.92269, 2.347, 2.4937, 5.0086, 3.3956, 3.9786, 3.6112, 0.9557, 2.1656, 2.4783, 1.7162, 1.3098, 3.4382, 0.67549, 0.53344, 3.8273, 4.5605, 1.8271, 2.5243, 2.4916, 1.4358, 1.4161, 2.4914, 1.8025, 2.5435, 1.7122, 2.5345, 2.5091, 1.3373, 4.5793, 2.4049, 6.4391, 2.7667, 2.4826, 4.3883, 3.8871, 4.3853, 3.073, 3.3666];

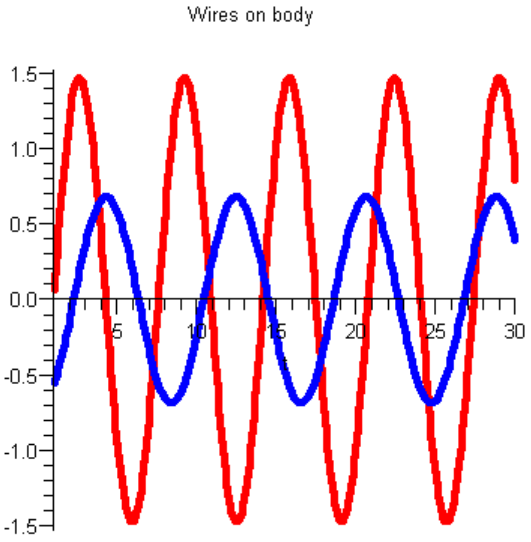

nwhh := [2.9902, 2.3461, 1.5768, 2.6801, 2.1605, 1.7474, 1.2864,
2.6163, 3.234, 3.546, 2.338, 3.8477, 2.2325, 3.5133,
3.5618, 2.5593, 2.3327, 2.1272, 1.6574, 2.1195, 3.5193, 2.8781,
1.5764, 1.4311, 3.2563, 3.2845, 2.564, 1.4189, 1.0782, 1.3227,
3.5949, 2.0295, 3.1405, 1.4265, 1.4768, 2.3642, 2.327, 2.0575,
1.0367, 2.6106, 3.4525, 2.6518, 2.4876, 2.4157, 4.0245,
0.87177, 2.7099, 2.25, 3.2173, 2.7642];

nwxdata := [1, 2, 3, 4, 5, 6, 7, 8, 9, 10, 11, 12, 13, 14, 15, 16, 17, 18, 19, 20, 21, 22, 23, 24, 25,
26, 27, 28, 29, 30, 31, 32, 33, 34, 35, 36, 37, 38, 39, 40, 41,
42, 43, 44, 45, 46, 47, 48, 49, 50];

Figure 8. Waves with wires on person

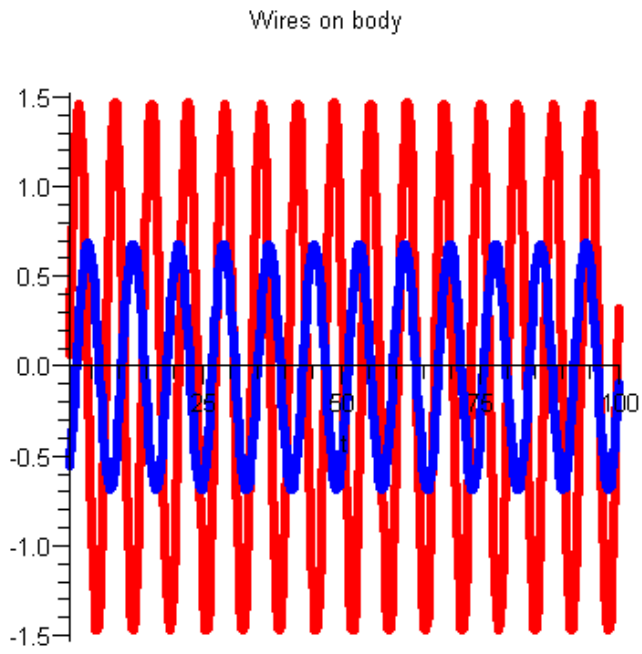

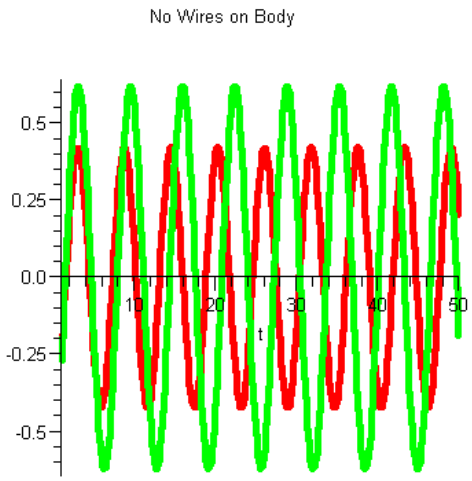

Figure 10. Waves with no wires on person

Figure 9. Waves with wires on person

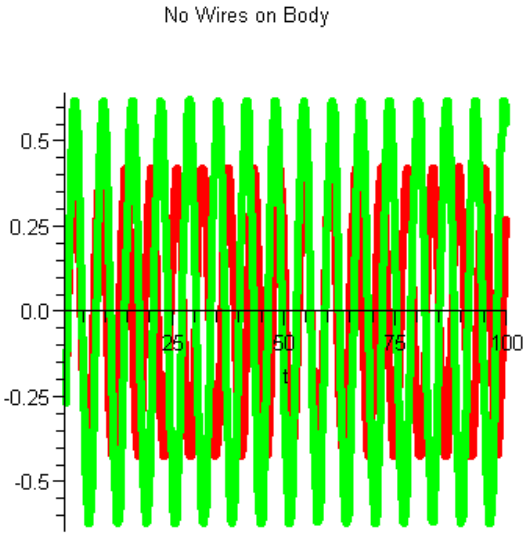

Figure 11. Waves with no wires on person

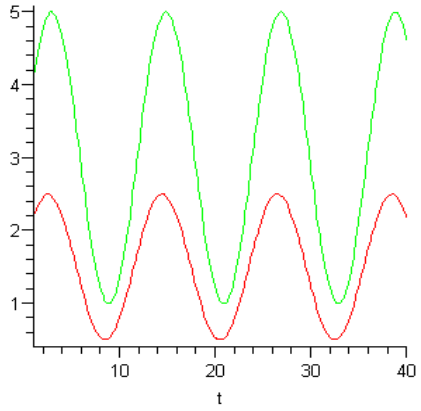

.
Figure 12. No wires on person.

The bottom line from analysis, confirmed with hypothesis testing at ***α=0.05,*** of these plots of the sinusoidal regression are:
For persons wearing wires the periodicity is different while for persons without wires the periodicity is the approximately the same.

3. INDICATORS FOR METRICS FOR DETECTION (INFORM DETECTION)

3.1 DETECTION METHODS and METRICS

Previously, we examined the absolute differences and the ratio of polarization. Now we move on to new constructs. Signal-to-noise ratios has been shown to be useful in detection and lowering false positives as shown by Kingsley et al (1992).

Our definition of SNR is shown is equation 1:

$$SNR = \frac{\mu}{\sigma}. \qquad (1)$$

Rather that look at this metric alone, we devise a ratio of SNR ratios for polarization wave forms. Our new metrics are shown in equations 2 and 3 below:

$$dm_1 = \frac{\frac{\mu_{vv}}{\sigma_{vv}}}{\frac{\mu_{HH}}{\sigma_{HH}}} \qquad (2)$$

or

$$dm_1 = \frac{\frac{\mu_{vv}}{\sigma_{vv}}}{\frac{\mu_{HH}}{\sigma_{HH}}} = \frac{\mu_{vv}\sigma_{HH}}{\mu_{HH}\sigma_{vv}} \qquad (3)$$

For example, for a person without wires on their person this calculation leads to

$$dm_1 = \frac{\frac{\mu_w}{\sigma_w}}{\frac{\mu_{HH}}{\sigma_{HH}}} = \frac{\mu_w\sigma_{HH}}{\mu_{HH}\sigma_w} = \frac{2.44 \cdot 0.83779}{2.36857 \cdot 1.35613} = 0.637069.$$

For persons wearing wires for detonation purposes, we have

2.7757.8206/(1.824*1.1267)= 1.10773.*

The values are both different and are significant using a level of significance of *a = 0.05*.

3.2 Levels of Detection

Level 1 Detection

We introduce a concept of Level 1 detection using radar only. Level 1 detection stem from a combination of output from radar capabilities. We use the following metrics for my support matrix in Table 1:

Metric 1: $M1=|VV_{mean}-HH_{mean}|$

Metric 2: $M2= \frac{VV_{mean}}{HH_{meam}}$

Metric 3: $dm_1 = \frac{\frac{\mu_{vv}}{\sigma_{vv}}}{\frac{\mu_{HH}}{\sigma_{HH}}} = \frac{\mu_{vv}\sigma_{HH}}{\mu_{HH}\sigma_{vv}}$

Metric 4: M4 = Periodicity of the polarizations scaling weighting (same=0, weak=.5, different=1)

Table 1. Detection Levels

Radar Scan				
Metric 1	M1			
Metric 2	0	M2		
Metric 3	0	0	dm1	
Metric 4	0	0	0	M4

The product of these values along the main diagonal yield a strength measure of the level 1 detection:

$$Detection\ \ level = M1 \cdot M2 \cdot M3 \cdot M4$$

The interpretation is as follows:
Detection Level =0 (not a person of interest)
Detection level > 0 (a person of interest)
The larger the value the higher the interest.
M1 usually has to be greater than 0.6, M2 greater than 1.35, dm1 greater than 1 or a Detection Level > 0.8 units.

Simulation models for Level 1 detection finds the following statistics supporting our claim in Table 2. We ran the model 824,000 trials.
Table 2. Simulation Results

	P(Success)	*P(False Success)*
Mean	*0.96189*	0.092336
Stand error	*0.00202*	0.004426
Median	*0.970508*	0.0808
St. Deviation	*0.02864*	0.0626
Minimum	*.875*	0
Maximum	*1*	0.303
Count	*824,000*	824,000
95% CI length	0.00399	0.0087

P(Successful detection) is about. 0.96189 and P(False Positives) is about 0.092336.

Level 1 detection shows us that we have a good success rate but still need a little improvement as well as improvement is needed in the false detections. Level 1 detection is based on single radar.

Multiple radars operating in independently and orthogonal in direction (if feasible) provides the best improvement. This will improve our *p(detection)* to greater than 99.84%. The *P(False Detections)* is reduced to less than 1% ≈ 0.85%.

Further improvement can be made with Level 2 and Level 3 Detections described next.

Level 2 Detection

We move on to using radar and video together. We take the level detection probabilities and combine with video of the crowd. Our video portion is examining for several quick indicators that will enhance the probabilities for detection and for false positives. Video indicators coupled after We get a Level 1 detection would include:

(1) folds or shape in clothing over suicide vests which have been clearly modeled by previous people.
(2) More clothing than needed based on weather and climate
(3) Sweat or massive perspiration not caused by climate
(4) Motion not consistent with others (saying when walking)

Each of these will be Bernoulli variable (1 if positive or 0 if negative). Any one positive indicator yields a 1 for the total. We total the values of each giving us a scale from 0 to 4.
The more one's the stronger the multiplier is for the detection.

We create a Level 2 detection metric:

$$L2DM = p(success\ from\ Level1) \square \sum Indicators$$

Video will most likely be used when then we have a probability flag for a suicide bomber. The video feed then is observed and processed by a computer program for abnormal traits of movement. We use the information as we showed previously in figure 2.

Level 3 Detection

Level 3 detection concerns using the radar to measure speed of the suspect. This can be done simultaneously with the other 2 detection strategies. We will use the work done by the Bornstein's on "Pace of Life" to measure discrepancies from the norm based on the findings of the FBI that the two suicide bombers caught were under the influence of drugs that modified their speed and perceptive abilities. First, in a region of concern we want to measure the typical speed of movement under normal circumstances. The radar gun is keyed to pick up a plus or minus one standard deviation changes in the normal speed as a flag indicator. This flag is coupled with either a strong Level 1and/or a Level 2 indicators to better detect the person wearing wires as a suicide bomber. We use three sensors (radar cross section (RCS), video, and radar speed) for my calculations for the probability of detection.

$$P(A \cup B \cup C) = P(A) + P(B) + P(C) - P(A) \cdot P(B) -$$
$$P(A) \cdot P(C) - P(B) \cdot P(C) + P(A) \cdot P(B) \cdot P(C)$$

for three events.

In our simulations introducing speed we find that speed needs to be coupled with other indicators to raise

its ability to predict. In a simulation model with the use of single radar with metrics discussed earlier only raised the probability of detection to approximately 100% and lowered the probability of false positive to approximately 0.5%.

Level 4 Detection

We consider more sensors in this level of detection to include thermal imagery and terahertz radar. My advanced algorithm uses Bayesian statistical updating analysis in order to calculate the probabilities of detection based on scans and visual sightings of the persons on interests.

For more than three events we use the inclusion - exclusion principle and the general form for four sensors of:

$$P(A_1 \cup A_2 \cup ... \cup A_4) = P(A_1) + P(A_2) + ... + P(A_4) - \sum_{i \neq j} P(A_i \cap A_j) + P(A_1 \cap A_2 \cap A_3) + P(A_1 \cap A_2 \cap A_4) + P(A_2 \cap A_3 \cap A_4) + P(A_1 \cap A_3 \cap A_4) - P(A_1 \cap A_2 \cap A_3 \cap A_4)$$

For the general case of the principle, let P(A_1), ..., P(A_n) be finite sets of Probabilities.

$$|\bigcup_{i=1}^{n} P(A_i)| = \sum_{i=1}^{n} P(A_i) - \sum_{i,j:1 \le i < j \le n} P(A_i \cap A_j) + \sum_{i,j,k:1 \le i < j < k \le n} P(A_i \cap A_j \cap A_k) - ... + (-1)^{n-1} P(A_i \cap ... \cap A_n)$$

Each sensor adds to the probability of detection and decreases the probability of a false detection.

More metrics considered

We experimented with phased metrics using metrics (a) through (d) that proved to better than a single metric alone. By phased metric we mean using more than one metric in the algorithm, i.e., using two or more radar RCS metrics in the detection scheme. In a simulation, we achieved a probability of detection of approximately 99%.

The sensitivity of the device (radar) and the collection apparatus is critical. The threshold values chosen are vital to the detection algorithm. For example, the higher the probability the further away from the mean the statistic is (see our figure below). Therefore, the SE now becomes an essential element.

Only data was used from identical subjects. We determine the following baseline data shown in Table 3 and Table 4:

Table 3. Baseline data for polarization differences

Status	Polarization	Mean	SD	1 SD Range
No wires	VV	2.44	.19	2.23,2.63
	HH	2.37	.11	2.26,2.48
	|VV-HH|	**0.09**	**.3**	**-.21,.39**
Wires (no loop)	VV	2.78	.19	2.57,2.97
	HH	1.83	.11	1.72,1.94
	|VV-HH|	**0.95**	**.30**	**0.65,1.25**
Wire (loop)	VV	2.87	.16	2.71,3.03
	HH	2.00	.17	1.83,2.17
	|VV-HH|	**0.87**	**0.33**	**0.54,1.20**

Table 4. Baseline data for polarization ratios

Status	Ratio VV/HH	Mean	SD	1 SD Range	3 SD Range
No wires	VV/HH	1.03	.12	.91,1.15	.67,1.37
Wires (no loop)	VV/HH	1.52	.15	1.37,1.67	1.07,1.97
Wires (loop)	VV/HH	1.43	.11	1.32,1.54	1.12,1.76

From a probabilistic standpoint we see that at 3 SD there is some slight overlap of values between no wires and wires in this case which are our false positives come from using only one sensor.

Enhancing our simulation to take advantage of this we find much improved results. Using both metrics together in a series fashion, the |VV-HH| and VV/HH, We found 100% of the bombers over a wider range of threshold values. We also am able to reduce the false positives to approximately 10-15%.

Video is an integral component to improve on detection. Video obtain simultaneous input that is couple with the radar infusion as shown is figure 2:

The radar becomes Flag 1 when it identifies through the combination of metrics above as potential subject. The video then analyzes the subject for deviations from the norm, approximately 1 SD. This becomes Flag 2. Two flags increase the probability of detection substantially. Adding a speed component to the radar is easy. Speed becomes the Flag 3 using the work done by the Bornstein's (1976) in walking speed of a crowd in world cities. Again, speeds that differ by approximately 1 SD are deemed critical. If all three flags are persistent then our probability of detection is over 99% and the false positive detections are less than 1% as evidence by simulation models.

Further, the addition of Thermal imagery can provide significant advantages. If the video camera or other surveillance device is added with thermal capability then we can measure the temperature change in a person. Significant temperature changes indicate that cold, hard substances are present that are different than 98.6^{o}. Again we look for 1 SD from the mean to

create a flag. This flag help increase the probability of detection as well as decrease the probability of a false detection.

Thus, adding the other sensors, speed and video, help reduce the percentages of false positives as well as the use of thermal imagery and increases our probability of a valid detection.

The detection algorithm for a real device will be realistic modification of the simulation algorithm below:

INPUTS: N, number of runs, assumed distribution for the number of suicide bombers in a crowd, distributions for probability metric for radar detections, threshold value
OUTPUTS: the number of positive detections, the number of false detections

Step 1. Initialize all counters: detections = 0, false alarms=0, suicide bombers =0
Step 2. For i = 1,2,…, N trials do
Step 3. Generate a random number from an integer interval [a,b].
Step 4. Obtain an event of a suicide bomber based upon our hypothesized distribution of the number of suicide bombers in a crowd of size X. Basically if random number $\leq$ *a specified small value* then I have a suicide bomber, otherwise I do not.
For example, I might generate random numbers between [1,300] and if the random number is ≤ 2 then the random number represents a suicide bomber.
Step 5. Generate characteristics for each person in the crowd by either being a bomber with random bomber characteristics or a non-bomber with random non-bomber characteristics based upon updated data collection feedback loop. I want to create a smart system.
Step 6. Allow the sensors to randomly detect the measures from Step 5 and use Step 7 to identify the characteristics based upon the metric used.
These distributions are described previously.
Step 7. Compare results from step 5-step 6 to threshold value using the following:
Target present: $y(t) > Y$→ correct detection
Target present: $y(t) < Y$→ missed detection
Target not present: $y(t) > Y$→ false alarm
Target not present: $y(t) < Y$→ no action
Step 8. For each correct detection, obtain a video and a speed input. Generate a random speed for each of the N trials above based upon Speed normal about 1 m/sec for a non-suicide bomber and Speed is 1-.5(rand( )) or 1+.5rand( ) for a bomber on drugs.
Step 9. Compare for detection with speed and video.
Target present: $z(t) > Z$→ correct detection
Target present: $z(t) < Z$→ missed detection
Target not present: $z(t) > Z$→ false alarm
Target not present: $z(t) < Z$→ no action

Step 10. If any are positive then use thermal imagery. Generate a random number for thermal imaging for temperature difference based upon

$$\frac{100\% \cdot (temperature_h - temperture_l)}{temperature_h}$$

Thermal difference for a normal person temperature percent differential of

$$\frac{100\% \cdot (temperature_h - temperture_l)}{temperature_h}$$ using

$temperature_h$= 98.6 and $temperture_l$ = 95

Thermal difference for a normal person temperature percent differential of

$$\frac{100\% \cdot (temperature_h - temperture_l)}{temperature_h}$$ using

$temperature_h$= 98.6 and $temperture_l$ = a random number between 70-95 degrees)

Step 11. Compare for detection by thermal imagining

Target present: $w(t) > W$→ correct detection
Target present: $w(t) < W$→ missed detection
Target not present: $w(t) > W$→ false alarm
Target not present: $w(t) < W$→ no action
Step 12. Increase all Counters as necessary
Step 13. Output statistics under the assumption of independence and use Inclusion-Exclusion as explained previously.

$$|\bigcup_{i=1}^{n} P(A_i)| = \sum_{i=1}^{n} P(A_i) - \sum_{i,j:1\le i<j\le n} P(A_i \cap A_j)$$
$$+ \sum_{i,j,k:1\le i<j<k\le n} [P(A_i \cap A_j \cap A_k) -$$
$$\ldots + (-1)^{n-1} P(A_i \cap \ldots \cap A_n)]$$

END of Algorithm

Figure 13. Simulation Algorithm for Methodology Model for RCS, Radar, Video, and Thermal Imagery

REFERENCES

Meigs, Montgomery C. Gen(Ret), 2007 JIEDDO PowerPoint Update Report to Congress, Director, Joint IED Defeat Organization, 19 November 2007.

Kingsley, S.,Quegan, S., 1992. *Understanding Radar Systems*, London, UK: McGraw Hill .

Bornstein, M H., Bornstein, H.G.,. 1976. The Pace of Life. *Nature*, 259, 557-559.

Angell A. ,Rappaport, C., 2007. Computational Modeling Analysis of Radar Scattering by Clothing Covered arrays of Metallic Body-Worn Explosive Devices", *Progress In Electromagnetics Research***,** PIER 76, 285–298.

Fox, W. P.,Vesecky, J., Laws,K. 2010. Detecting Suicide Bombers, *Journal of Defense Modeling and Simulation (JDMS)*, pp 1-20

Dogaru, T.,Nguyen,L. Le, C., 2007. Computer models of the human body signature for sensing through the wall radar applications, Tech. Rpt. ARL-TR-4290, Army Research Laboratory .

Fox, W.P.,Giordano, F., Horton, S., Weir, M. 2009. *A First Course in Mathematical Modeling*, 4th Ed. Belmont: Cengage Publishing.

Fox, W.P., 2012. *Mathematical Modeling with Maple*, Belmont: Cengage Publishing.

AUTHORS BIOGRAPHY

Dr. William P. Fox is a professor in the Department of Defense Analysis at the Naval Postgraduate School. He received his BS degree from the United States Military Academy at West Point, New York, his MS at the Naval Postgraduate School, and his Ph.D. at Clemson University. Previous he has taught at the United States Military Academy and Francis Marion University where he was the chair of mathematics for eight years. He has many publications including books, chapters, journal articles, conference presentations, and workshops. He directs several math modeling contests through COMAP. His interests include applied mathematics, optimization (linear and nonlinear), mathematical modeling, statistical models for medical research, and computer simulations. He is Vice-President of the Military Application Society in INFORMS.

Professor John Vesecky studied Electrical Engineering at Rice University before attending graduate school at Stanford. After academic posts at the University of Leicester UK, Stanford and Michigan he was selected in 1999 as Founding Chairman of the Electrical Engineering Department in the new Jack Baskin Engineering School at the University of California, Santa Cruz. He has served as Chair or Associate Chair ever since. Recent teaching experience has focused on Capstone Design Courses for undergraduates and the impact of technological innovation on environmental challenges. In the 1990s he served on Vice-President Gore's Environmental Task Force as Chair of the Sensors Panel. His areas of research expertise include radar and radar systems, Earth remote sensing, ocean sensors and autonomous vehicles. He has a lifelong interest in amateur radio and holds an amateur extra class FCC license, AE6TL. He is an IEEE Fellow.

Adjunct Professor Kenneth Laws studied Physics at the University of California, finishing with a Doctorate in 2001. Since then he has done research on topics in radar applications to ocean remote sensing, emphasizing the use of HF (decameter wavelength) radars along the coast line to measure ocean currents. The main thrust of his research has been the analysis of errors in surface current measurements and tracking ships using HF radar. He has also worked with autonomous ocean surface vehicles and renewable energy projects in the coastal environment. His teaching experience includes engineering design classes and bringing the engineering and science aspects of sustainable energy to a wide spectrum of undergraduate students.

I